Scientific paper

A Facile Synthesis of Bioactive Five- and Six-membered *N*-heterocyclic Aromatic Compounds Using $AlCoFe_2O_4$ as a Green Catalyst

Fatemeh Mostaghni, Homa Shafiekhani and Nosrat Madadi Mahani

Department of Chemistry, Payame Noor University, P.O. Box 19395-4697 Tehran, Iran

** Corresponding author: E-mail: mostaghnif@yahoo.com*

Received: 06-19-2021

Abstract

Nitrogen-containing heterocycles have been extensively studied due to their broad biological and pharmaceutical applications. In this study, we synthesized five- and six-membered nitrogen-containing rings through one-pot multicomponent reaction using an aluminium-doped cobalt ferrite nano-catalyst. The nano-catalyst was prepared by the co-precipitation method from the corresponding metal salts. The obtained results show that the proposed catalyst has a high efficiency and has enabled the formation of the desired products with high efficiency and purity. In addition, simplicity of operation, facile purification of products, shorter reaction times, mild reaction conditions, easy separation and recyclability of the catalyst, are the main advantages of this catalyst.

Keywords: Green catalyst; magnetic nano-catalyst; *N*-heterocyclic aromatic compounds; one-pot multicomponents reactions

1. Introduction

Heterocyclic compounds have significant importance in medicinal chemistry.[1–3] Among them, nitrogen-containing heterocycles, are the most important heterocyclic moieties of choice for the many bio-active compounds.[4–6]

In recent years, imidazoles, benzimidazoles and pyridines are subject of intense investigations because of their wide biological and pharmaceutical applications. Numerous biological activities have been described for imidazole derivatives such as anti-viral, antimicrobial, antifungal, anti-tumor, anti-tubercular, and anti-inflammatory activities.[7–18] These compounds contain two nitrogen atoms placed at 1 and 3 position in their ring structure, which possesses both acidic and basic characteristics. Since both nitrogen atoms can carry hydrogen atom, these compounds appear in two tautomeric forms. In addition, imidazole moieties are very polar compounds, and possess affinity towards enzymes and protein receptors.[19]

Also, medicinal properties of pyridin ring, particularly 2,4,6-triarylpyridines known as Krohnke pyridines, include antimalarial, anaesthetic, antiparasitic, and antitumor activity, as well as agents that are used for photodynamic cell specific cancer therapy.[20–23]

In the past few decades, various methods included synthesis performed by various metal oxide catalysts in the presence or absence of a solvent as well as microwave-assisted synthesis, have been reported for the synthesis of imidazoles,[24–29] and Krohnke pyridines.[30–37]

In recent years, there has been increasing interest to develop a simple, efficient and eco-friendly, benign organic transformations catalyzed by cheap and recyclable metals or their salts, avoiding the harmful and pollutant conditions.

In this study, heterogeneous $AlCoFe_2O_4$ nanocatalyst was used as a suitable catalyst in one-pot multi-component reactions for preparation of bioactive five- and six-membered *N*-heterocyclic aromatic compounds. This catalyst was considered suitable for this purpose due to mild reaction conditions, short reaction times, easy separability and recyclability of the catalyst.

In addition, $AlCoFe_2O_4$ nano-particles have high saturation magnetization, strong anisotropy, high coercivity and excellent physiochemical stability.[38–41]

Many preparation methods for $AlCoFe_2O_4$ nano-particles have been reported, such as the ball milling, co-precipitation, hydrothermal synthesis, sol-gel, and reaction in a micro-emulsion.[42–46] Here, we synthesized the magnetic nano-catalyst ($AlCoFe_2O_4$) using co-precipitation method from metalic salts.

2. Experimental

2. 1. Material and Methods

All materials and reagents were purchased from Merck, and Aldrich and used without further purification. XRD patterns prepared using powder X-ray diffraction (Bruker diffractometer, Cu-Kα X-rays of wavelength λ = 1.5406 Å). Melting points of the synthesized compounds were determined on Electrothermal-9200 melting point apparatus. IR spectra was recorded on KBr Pellets by Shimadzu 8400S FT-IR spectrophotometer. ^{1}H and ^{13}C NMR spectra were recorded on a Bruker Advanced DPX spectrometer (400 MHz for ^{1}H NMR and 100 MHz for ^{13}C NMR). SEM image provided by the scanning electron microscope (FE-SEM, Mira3 Tescan). The absorption spectra was recorded on UV-VIS spectrophotometer (Perkin Elmer, Lambda 35).

2. 2. Synthesis of Nanocatalyst

$CoFe_{2-x}Al_xO_4$ nanocatalyst was prepared by the co-precipitation method from aqueous solutions of $CoCl_2$, $FeCl_3$ and aluminum nitrate. First, stoichiometric amounts of the three metallic salts were individually dissolved in 10 mL of deionized water. Then, the three metallic solutions were poured in the reaction vessel and stirred vigorous for 30 minutes at room temperature. Polyethylene glycol (average molecular weight: 4000, Qualigen) was then added to the above solution as a surfactant. Finally, the mixed solution was neutralized to pH 8 by drop-by-drop addition of 25% ammonia solution. The resulting solution was kept under stirring at 60 °C for 1 hour. The obtained particles were thoroughly washed several times with distilled water and filtered. Finally, the precipate was dried at 80 °C and calcined at 500 °C for 3 hours.

The synthesized nanocatalyst was characterized by powder X-ray diffraction (XRD), scanning electron microscopy (SEM-EDS), vibrating sample magnetometry (VSM), difuse reflectance and UV-vis spectroscopy.

2. 3. General Procedure for the Preparation of 2,4,6-Triphenylpyridines

Various amounts of nano-particle nanocatalyst were added to a stirred solution of acetophenones (2 mmol), aromatic aldehydes (1 mmol), and ammonium acetate (4 mmol). Then, the mixture was stirred at various temperatures under solvent-free condition. At the end of the reaction (monitored by TLC), the catalyst was separated using an external magnet and the reaction mixture was treated with ethanol to form crystals. The crude product was obtained by filtration and washed with ethanol. Purification of the crude product was performed by re-crystallization in ethanol.

Characterization data of selected compounds:

2,4,6-Triphenylpyridine (Table 3, entry 1)

IR (KBr): ν 3071, 1590, 1493, 1471, 1033, 871, 665 cm^{-1}; ^{1}H NMR (400 MHz, DMSO-d_6): δ 7.45–7.62 (m, 9H), 7.95 (d, J = 7.6 Hz, 2H), 8.19 (s, 2H), 8.24 (d, J = 7.5 Hz, 4H); ^{13}C NMR (100 MHz, DMSO-d_6): δ 117.17, 127.3, 127.5, 128.6, 128.9, 129.5, 130.1, 138.8, 139.4, 150.3, 157.4.

2,6-Bis(4-fluorophenyl)-4-phenylpyridine (Table 3, entry 2)

IR (KBr): ν 1601, 1595, 1506, 1421, 1330, 1223, 1160, 1116, 1075, 987, 825 cm^{-1}; ^{1}H NMR (400 MHz, DMSO-d_6): δ 7.37 (m, 5H), 7.51 (m, 2H), 8.13 (q, 2H), 8.23 (s, 2H), 8.32–8.41 (m, 4H); ^{13}C NMR (100 MHz, DMSO-d_6): δ 164.21, 161.67, 155.78, 155.53, 148.59, 148.52, 138.71, 134.96, 135.08, 134.12, 134.00, 129.68, 129.56, 129.27, 129.14, 128.86, 128.65, 126.87, 116.42, 116.26, 116.13, 115.89, 115.71, 115.56, 115.35.

2,6-Bis(4-fluorophenyl)-4-(4-chlorophenyl)pyridine (Table 3, entry 3)

IR (KBr): ν 1612, 1592, 1510, 1416, 1328, 1210, 1162, 1105, 1073, 994, 823 cm^{-1}; ^{1}H NMR (400 MHz, DMSO-d_6): δ 7.36 (m, 3H), 7.61 (m, 3H), 8.09 (m, 2H), 8.21 (s, 2H), 8.38 (m, 4H); ^{13}C NMR (100 MHz, DMSO-d_6): δ 164.21, 161.72, 155.49, 155.24, 154.98, 148.55, 137.43, 137.42, 135.12, 134.19, 133.94, 129.68, 129.50, 129.32, 129.13, 128.94, 128.59, 116.68, 116.45, 116.27, 116.12, 115.94, 115.72, 115.52, 115.31.

2,6-Bis(4-bromophenyl)-4-(4-fluorophenyl)pyridine (Table 3, entry 4)

IR (KBr): ν 1658, 1592, 1505, 1411, 1330, 1210, 1159, 1107, 1070, 997, 819 cm^{-1}; ^{1}H NMR (400 MHz, DMSO-d_6): δ 7.30 (t, J = 8.8 Hz, 2H), 7.72–7.82 (m, 5H), 7.88 (s, 1H), 7.92–8.02 (m, 4H), 8.10 (d, J = 8.4 Hz, 2H); ^{13}C NMR (100 MHz, DMSO-d_6): δ 116.3, 116.5, 122.0, 127.8, 131.0, 131.7, 131.72, 131.8, 131.9, 132.3, 136.9, 143.7, 162.7, 165.2, 188.6.

2,6-Bis(4-bromophenyl)-4-(4-methoxyphenyl)pyridine (Table 3, entry 5)

IR (KBr): ν 3008, 2937, 1665, 1596, 1511, 1463, 1329, 1309, 1261, 1219, 1175, 1037, 984, 819 cm^{-1}; ^{1}H NMR (400 MHz, DMSO-d_6): δ 3.81 (s, 3H), 7.05 (d, J = 8.2 Hz, 2H), 7.72–7.88 (m, 8H), 8.11 (d, J = 8.2 Hz, 4H); ^{13}C NMR (100 MHz, DMSO-d_6): δ 56.1, 115.2, 120.3, 128.1, 128.7, 131.3, 131.8, 132.4, 138.3, 145.5, 162.3, 189.1.

2. 4. General Procedure for the Preparation of 2,4,5-Triphenyl-1*H*-imidazoles

Various amounts of $AlCoFe_2O_4$ nanocatalyst were added to a stirred solution of aromatic aldehydes (1 mmol), benzoin (1 mmol), and ammonium acetate (4 mmol) in ethanol (10 mL). Then, the mixture was stirred at various temperature. At the end of the reaction (monitored by

TLC) the magnetic nanocatalyst was separated using an external magnet. Then, the reaction mixture was diluted with 50 mL of cold water. Finally, the crude product was collected by filtration and washed with EtOH. Purification of the crude product was performed by re-crystallization from acetone: water (9:1). Characterization data of selected compounds were as follow:

2,4,5-Triphenyl-1*H*-imidazole (Table 4, entry 1)

IR (KBr): ν 3445, 3082, 2853, 1641, 1504, 1462, 1398, 1128, 1070, 966, 766, 698 cm^{-1}; ^1H NMR (400 MHz, DMSO-d_6): δ 7.22 (dd, 1H, *J* = 7.2 Hz), 7.34 (dd, 2H, *J* = 7.2 Hz), 7.39 (dd, 2H, *J* = 7.2 Hz), 7.44–7.51 (m, 6H), 7.59 (d, 2H, *J* = 7.6 Hz), 8.10 (d, 2H, *J* = 7.2 Hz), 12.71 (br, 1H); ^{13}C NMR (100 MHz, DMSO-d_6): δ 125.2, 126.5, 127.0, 127.7, 128.1, 128.2, 128.3, 128.4, 130.3, 131. 0, 135.1, 137.1, 145.3.

2-(4–Chlorophenyl)-4,5–diphenyl–1*H*-imidazole (Table 4, entry 2)

IR (KBr): ν 3411, 3060, 2854, 1608, 1485, 1428, 1433, 1325, 1158, 833 cm^{-1}; ^1H NMR ($CDCl_3$): δ 12.76 (s, 1H), 7.84 (d, 2H, *J* = 8.6 Hz), 7.54 (d, *J* = 6.8 Hz 4H), 7.37–7.28 (m, 8H); ^{13}C NMR ($CDCl_3$): δ 144.82, 137.52, 135.19, 132.24, 130.83, 130.80, 129.24, 128.96, 128.54, 128.48, 128.49, 128.14, 127.15, 126.75, 126.34.

2-(4-Hydroxyphenyl)-4,5-diphenyl-1*H*-imidazole (Table 4, entry 3)

IR (KBr): ν 3438, 2964, 2828,1602, 1482, 1445, 1374, 1317, 1130, 1034, 968, 764, 692 cm^{-1}; ^1H NMR (400 MHz, $CDCl_3$): δ 12.51 (s, 1H), 7.20–7.52 (m, 10H), 6.99 (d, 2H, *J* = 7.8 Hz), 6.89 (d, 2H, *J* = 7.5 Hz); ^{13}C NMR ($CDCl_3$): δ 158.3, 156.55, 145.46, 129.18, 128.37, 127.93, 126.92, 124.74, 119.08, 116.54, 112.82.

2-(4-Methoxyphenyl)-4,5-diphenylimidazole (Table 4, entry 4)

IR (KBr): ν 1256, 1616, 2465, 2988, 3428 cm^{-1}; ^1H NMR (400 MHz, DMSO-d_6): δ 12.52 (s, br, 1H), 8.05 (d, *J* = 8.6 Hz, 2H), 7.50 (d, *J* = 6.3 Hz, 4H), 7.35 (m, 6H), 7.08 (d, *J* = 8.7 Hz, 2H), 3.83 (s, 3H); ^{13}C NMR (100 MHz, DMSO-d_6): δ 159.37, 145.81, 132.81, 127.84, 127.47, 126.56, 126.24, 123.13, 113.28, 54.45.

2-(4-Nitrophenyl)-4,5-diphenylimidazole (Table 4, entry 5)

IR (KBr): ν 3438, 3293, 2856, 1605, 1541, 1484, 1335, 1323, 1225, 1026, 838 cm^{-1}; ^1H NMR (400 MHz, DMSO-d_6) δ 7.45–7.52 (m, 2H), 7.74 (d, *J* = 4 Hz, 1H), 7.81–7.86 (m, 3H), 8.22–8.26 (m, 4H), 8.36–8.39 (m, 5H), 13.58 (s, 1H); ^{13}C NMR (100 MHz, DMSO-d_6) δ 159.2, 137.1, 133.2, 131.9, 131.2, 130.8, 129.2, 128.8, 128.6, 128.4, 128.1, 127.5, 127.1, 126.4, 126.1, 125.8, 124.3, 122.6.

3. Results and Discussion

3. 1. Characterization of the Nanocatalyst

Figure 1 shows the single-phase spinel nature of the synthesized nano catalyst was confirmed by the sharp peaks at 2θ (23.74, 29.89, 35.52, 43.14, 54.16, 57.10, 62.99), which are accredited to (111), (220), (311), (400), (422), (511) and (440). All the peaks were indexed within a single

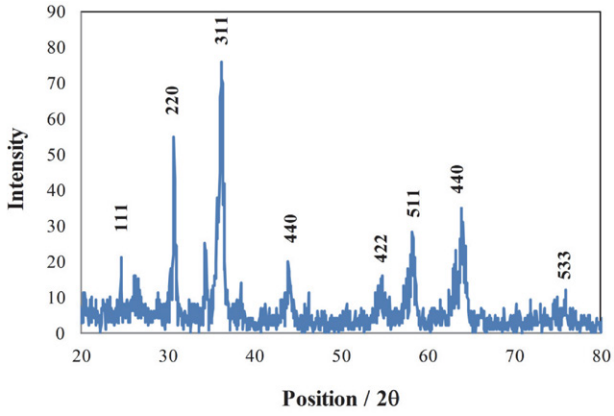

Figure 1. XRD patterns of $AlCoFe_2O_4$

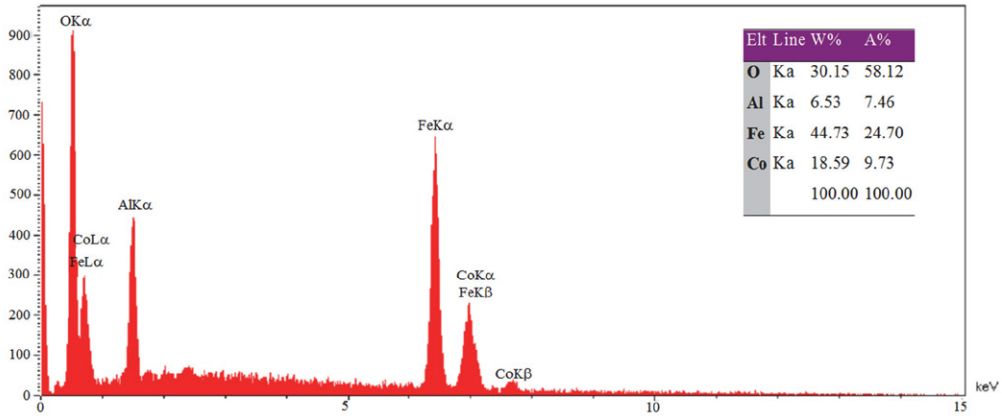

Figure 2. EDS of $AlCoFe_2O_4$

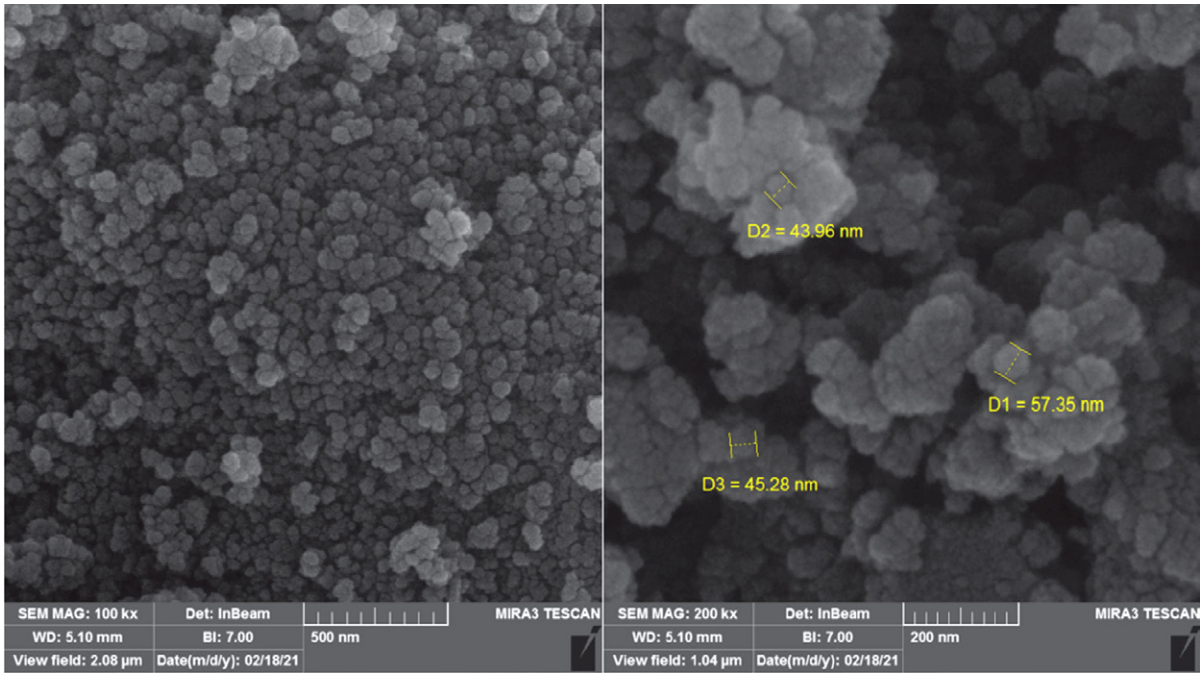

Figure 3. FESEM image of $AlCoFe_2O_4$ nanocrystals

phase cubic spinel structure with *Fd3m* space group (JCPDS Card No. 86-2267).

The crystallite size was calculated from intensity of the highly difracted peak (311) according to the Debye–Scherrer formula giving the crystal sizes of 6.63. To determine the elemental compositions of synthesized nanocatalyst, quantitative analysis was performed using EDS (Fig. 2). The obtained results approved the characteristic peaks of Al, Co, Fe, and O with 7.46, 9.73, 24.70 and 58.12 atomic percentage, respectively.

The above results indicated that the $AlCoFe_2O_4$ nanocatalyst has been successfully synthesized without any impurities. Figure 3 shows the microstructure of synthesized $AlCoFe_2O_4$ nanocrystals. As can be seen in this photograph, it was understood that the nanoparticles were cubic shape with an average diameter size less than 45 nm with some agglomeration. The cubic structure of spinel ferrites is mainly due to the lack of Co^{2+} ions at octagonal sites, which leads to the absence of co-operative active Jahn–Teller distortion.

Couplings at the atomic level, including the coupling between electron spins and between the electron spin and the angular momentum of the electron orbital are two factors that create magnetic properties in materials. Figure 4 showed the hysteresis loops of $AlCoFe_2O_4$ nanoparticles measured using a vibrating sample magnetometer (VSM).

As can be seen, the saturation magnetization (MS), the remanent magnetization (Mr) and coercivity (Hc) values obtained for the sample were 18.05 emu/gr, 394 Oe, and 4.44 emu/gr, respectively. The low values of remanent magnetization and coercivity of the nanoparticles are consistent with the properties of the soft magnetic material. Diffuse

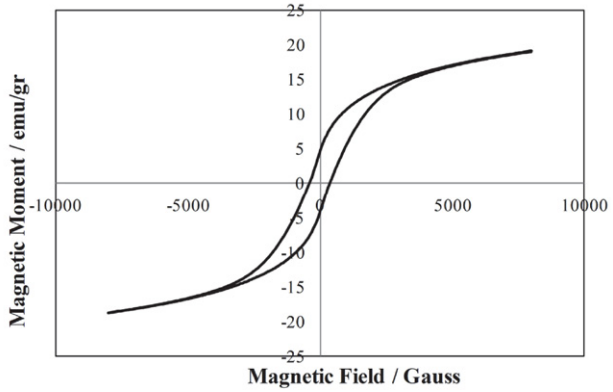

Figure 4. Hysteresis loop of $AlCoFe_2O_4$ nanoparticles

reflectance (DRS) and UV-vis spectra of the sample were obtained using a V-670, JASCO spectrophotometer. DRS spectra of synthesized nanocatalyst is shown in Figure 5.

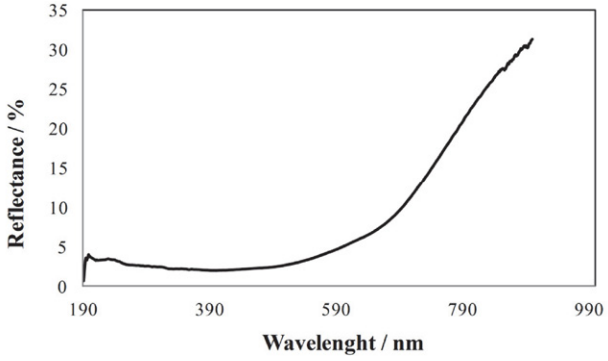

Figure 5. Diffuse reflectance spectra of $AlCoFe_2O_4$ nanocatalyst

As can be seen in the Figure 5, the synthesized nanocatalyst exhibited high value of diffuse reflectance percentage. The energy band gap of photocatalyst is determined using the absorption spectra according to the Tauc equation as follow:

$$(\alpha h\nu) = \beta\left(h\nu - E_g\right)^{\frac{n}{2}}. \quad (1)$$

Where α is the absorption coefficient, β is the absorption constant and E_g is the energy gap. The value of n for the direct optical gap is 1. According to Figure 6, the direct optical gap value is 1.43 ev.

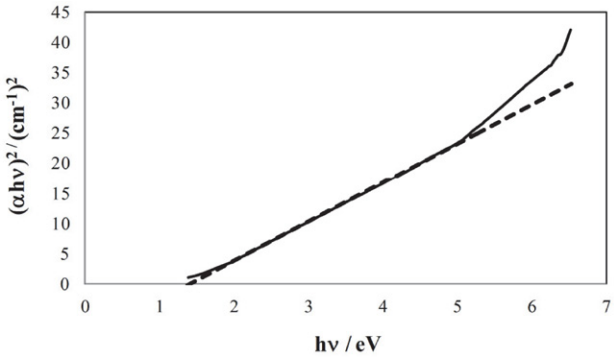

Figure 6. Plot $(\alpha h\nu)^2$ vs. photon energy (inset) of $AlCoFe_2O_4$ nanocatalyst

3. 2. Evaluation of Catalytic Properties

To evaluate the catalytic properties of the synthesized nanoparticles, the synthesis of pyridine and imidazole derivatives through one-pot three-component condensation was selected as the model reaction. Catalytic efficiency and optimal reaction conditions were evaluated by performing reactions at different temperatures and applying different amounts of nanocatalysts. The first derivative in each reaction was selected as the representative to optimize this reaction. The results are presented in Tables 1 and 2.

The results presented in Table 1 clearly show that at 120 °C and in the presence of 15 mol% of the catalyst, the reaction 1 led to the formation of triphenylpyridine at short reaction time and in high yield. It was also found that further increase in temperature led to a decrease in efficiency. This can be related to the possibility of side reactions. According to the results presented in Table 1, further increases in the amount of the catalyst did not have any significant effect on the reaction time and efficiency.

However, reaction 2 was also completed immediately and the pure product was obtained simply by recrystalliz-

Table 1. Optimization of reaction conditions for preparing 1,3,5-triphenylimidazole

Entry	Catalyst (mol%)	*T* (°C)	Time	Yield (%)
1	None	r.t	10 h	–
2	None	50	10 h	trace
3	None	80	10 h	19
4	2	r.t	5 h	35.5
5	2	50	10 min	53
6	2	80	10 min	49
7	5	r.t	5 h	83.5
8	5	50	10 min	98
9	5	80	10 min	78.5
10	7	r.t	5 h	84
11	7	50	10 min	99
12	7	80	10 min	73

Table 2. Optimization of reaction conditions for preparing 2,4,6-triphenylpyridine

Entry	Catalyst (mol%)	*T* (°C)	Time	Yield (%)
1	7	80	3 h	–
2	7	100	3 h	23
3	7	120	3 h	67
4	10	80	3 h	34
5	10	100	3 h	64
6	10	120	3 h	91
7	15	80	3 h	52
8	15	100	3 h	75
9	15	120	3 h	97
10	20	80	3 h	54
11	20	100	3 h	79
12	20	120	3 h	98

Table 3. Preparation of 2,4,6-triarylpyridine derivatives using $AlCoFe_2O_4$ nanocatalyst

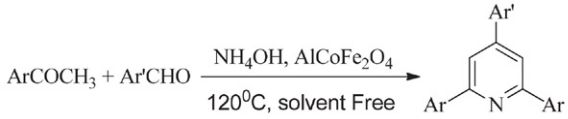

Entry	Ar	Ar‘	Time (min)	yield (%)	m.p. (°C)
1	Ph	Ph	60	97	135–137
2	4-F-C_6H_4-	Ph	60	95	174–176
3	4-F-C_6H_4-	4-Cl-C_6H_4-	90	94	224–226
4	4-Br-C_6H_4-	4-F-C_6H_4-	90	96	148–150
5	4-Br-C_6H_4-	4-OMe-C_6H_4-	60	98	177–189

Table 4. Preparation of 2,4,5-triarylimidazole derivatives using $AlCoFe_2O_4$ nanocatalyst

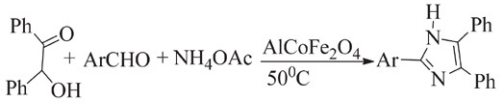

Entry	Ar	Time (min)	Yield (%)	m.p. (°C)
1	Ph	10	97	277–278
2	4-Cl-C_6H_4-	15	92	256–258
3	4-OH-C_6H_4-	10	98	268–270
4	4-OMe-C_6H_4-	10	98	230–232
5	4-NO_2-C_6H_4-	20	92	255–257

ing from ethanol without the need for any chromatographic technique. Table 2 shows that the optimal conditions were obtained with 5 mol% of catalyst at 50 °C. The reaction yield did not increase significantly with increasing the amount of catalyst. However, the reactions with the other benzaldehyde derivatives and aromatic ketones was investigated to develop the method. The results are presented in Tables 3 and 4.

The results indicate that the performance of the catalyst was efficient without the formation of by-products with the wide range of aromatic aldehydes containing electron acceptor and electron donor substituents. In general, this catalyst has produced pure products with high efficiency at short reaction times and low reaction temperatures which makes this catalyst economically and environmentally useful. Furthermore, the catalyst was also successfully recycled and used for at least 5 times without significant reduction in catalytic activity. We believe that the proposed catalyst is a green and efficient catalyst compared to the previously reported different catalysts.

4. Conclusion

In this research, we synthesized aluminum-doped cobalt ferrite nanocatalyst using co-precipitation method. The characterization results showed that the nanoparticles were cubic shape with an average diameter size less than 45 nm with some agglomeration. The low remanent magnetization and coercivity of the nanoparticles are consistent with the properties of the soft magnetic material. Furthermore, the prepared nanoparticles were used as an effective green catalyst for one-pot multicomponent reactions. The results showed that the synthesized nanoparticles were able to create the desired heterocycle products with high efficiency and purity. In both types of reactions, a wide range of acetophenones and aromatic aldehydes containing electron acceptor groups as well as electron donor groups on the aromatic ring provided the desired products at good isolated yields. In addition, simplicity of operation, facile purification of products, shorter reaction times, mild reaction conditions, easy separation and recyclability of the catalyst, were the main advantage of this catalyst.

Acknowledgments

We are grateful to Payam Noor University for encouragements.

5. References

1. E. El-Sayed, A. Fadda, A. El-Saadaney, *Acta Chim. Slov*. **2020**, *67*, 1024–1034. **DOI:**10.17344/acsi.2019.5007
2. G. H. Elgemeie, R. A. Mohamed, *Heterocycl. Commun*. **2014**, *20*, 257–269. **DOI:**10.1515/hc-2014-0156
3. J. R. Vishnu, A. Sethi, R. Pratap, *The Chemistry of Heterocycles*, 1st Ed. Elsevier, Amsterdam, **2019**
4. H. Beyzaei, S. Sargazi, G. Bagherzade, A. Moradi, E. Yarmohammadi, *Acta Chim. Slov*. **2021**, *68*, 109–117. **DOI:**10.17344/acsi.2020.6208
5. T. Chaban, J. Matiychuk, O. Shyyka, I. Chaban, V. Ogurtsov, I. Nektegayev, V. Matiychuk, *Acta Chim. Slov*. **2020**, *67*, 1035–1043. **DOI:**10.17344/acsi.2019.5439
6. F. Tok, B. Koçyiğit-Kaymakçıoğlu, Design, *Acta Chim. Slov*. **2020**, *67*, 1139–1147. **DOI:**10.17344/acsi.2020.6028
7. K. Bhandari, N. Srinivas, V. K. Marrapu, A. Verma, S. Srivastava, S. Gupta, *Bioorg. Med. Chem. lett.* **2010**, *20*, 291–293 **DOI:**10.1016/j.bmcl.2009.10.117
8. R. Thomas, M. Hossain, Y. S. Mary, K. S. Resmi, S. Armaković, S. J. Armaković, A. K. Nanda, V. K. Ranjan, G. Vijayakumar, C. Van Alsenoy, *J. Mol. Struct*. **2018**, *1158*, 156–175. **DOI:**10.1016/j.molstruc.2018.01.021
9. A. Gomtsyan, *Chem. Heterocycl. Comp*. **2012**, *48*, 7–10. **DOI:**10.1007/s10593-012-0960-z
10. X. Lu, X. Liu, B. Wan, S. G. Franzblau, L. Chen, C. Zhou, Q. You, *Euro. J. Med. Chem*. **2012**, *49*, 164–171. **DOI:**10.1016/j.ejmech.2012.01.007
11. N. Nagarajan, G. Vanitha, D. A. Ananth, A. Rameshkumar, T. Sivasudha, R. Renganathan, *J. Photochem. Photobiol. B.* **2013**, *127*, 212–222. **DOI:**10.1016/j.jphotobiol.2013.08.016
12. T. C. Chen, D. S. Yu, K. F. Huang, Y. C. Fu, C. C. Lee, C. L. Chen, F. C. Huang, H. H. Hsieh, J. J. Lin, H. S. Huang, *Euro. J. Med. Chem*. **2013**, *69*, 278–293. **DOI:**10.1016/j.ejmech.2013.06.058
13. X. D. Yang, W. C. Wan, X. Y. Deng, Y. Li, L. J. Yang, L. Li, H. B. Zhang, *Bioorg. Med. Chem. Lett*. **2012**, *22*, 2726–2729. **DOI:**10.1016/j.bmcl.2012.02.094

14. L. Xiaojing, J. Yanrong, J. Hao, G. Guanlei, X. Min, *Acta Chim. Sinica*, **2019**, *77*, 1194–1202.
15. M. Smitha, Y.S. Mary, M. Hossain, K. S. Resmi, S. Armaković, S. J. Armaković, R. Pavithran, A. K. Nanda, C. Van Alsenoy, *J. Mol. Struct*. **2018**, *1173*, 221–239. **DOI:**10.1016/j.molstruc.2018.06.110
16. E. Vessally, S. Soleimani-Amiri, A. Hosseinian, L. Edjlali, A. Bekhradnia, *Rsc Advances,* **2017**, *7*, 7079–7091. **DOI:**10.1039/C6RA25816F
17. Y. Bansal, R. Minhas, A. Singhal, R. K. Arora, G. Bansal, *Curr. Org. Chem*. **2021**, *25*, 669–694. **DOI:**10.2174/1385272825666210208141107
18. M. Gaba, C. Mohan, *Med. Chem. Res*. **2016**, *25*, 173–210. **DOI:**10.1007/s00044-015-1495-5
19. M. A. Chiacchio, D. Iannazzo, R. Romeo, S. V. Giofrè, L. Legnani, *Curr. Med. Chem*. **2019**, *26*, 7166–7195. **DOI:**10.2174/0929867325666180904125400
20. S. Prachayasittikul, R. Pingaew, A. Worachartcheewan, N. Sinthupoom, V. Prachayasittikul, S. Ruchirawat, V. Prachayasittikul, *Mini Rev. Med. Chem*. **2017**, *17*, 869–901. **DOI:**10.2174/1389557516666160923125801
21. D. Im, K. Jung, S. Yang, W. Aman, J. M. Hah, *Euro. J. Med. Chem*. **2015**, *102*, 600–610. **DOI:**10.1016/j.ejmech.2015.08.031
22. G. H. Elgemeie, R. A. Mohamed, *Heterocycl. Commun*. **2014**, *20*, 257–269. **DOI:**10.1515/hc-2014-0156
23. M. Hossain, A. K. Nanda, *Sci. J. Chem*. **2018**, *6*, 83–94.
24. A. A. Napoleon, F. R. Khan, E. D. Jeong, E. H. Chung, *Chin. Chem. Lett*. **2015**, *26*, 567–571. **DOI:**10.1016/j.cclet.2015.01.008
25. A. R. Moosavi-Zare, Z. Asgari, A. Zare, M. A. Zolfigol, M. Shekouhy, *RSC Advances,* **2014**, *4*, 60636–60639. **DOI:**10.1039/C4RA10589C
26. D. Tang, P. Wu, X. Liu, Y. X. Chen, S. B. Guo, W. L.Chen, J. G. Li, B. H. Chen, *J. Org. Chem*. **2013**, *78*, 2746–2750. **DOI:**10.1021/jo302555z
27. C. Y. Chen, W. P. Hu, P. C. Yan, G. C. Senadi, J. J. Wang, *Org. Lett.* **2013**, *15*, 6116–6119. **DOI:**10.1021/ol402892z
28. H. R. Shaterian, M. Ranjbar, *J. Mol. Liq*. **2011**, *160*, 40–49. **DOI:**10.1016/j.molliq.2011.02.012
29. Z. J. Cai, S. Y. Wang, S. J. Ji, *Org. Lett*. **2012**, *14*, 6068–6071. **DOI:**10.1021/ol302955u
30. H. Alinezhad, M. Tajbakhsh, N. Ghobadi, *Synth. Commun*. **2015**, *45*, 1964–1976. **DOI:**10.1080/00397911.2015.1041046
31. Z. Zarnegar, J. Safari, M. Borjian-borujeni, *Chem. Heterocycl. Compd*. **2015**, *50*, 1683–1691. **DOI:**10.1007/s10593-015-1638-0
32. Y. M. Ren, Z. Zhang, S. Jin, *Synth. Commun*. **2016**, *46*, 528–535. **DOI:**10.1080/00397911.2016.1152375
33. D. S. Rekunge, I. A. Kale, G. U. Chaturbhuj, *J. Iran. Chem. Soc*. **2018**, *15*, 2455–2462. **DOI:**10.1007/s13738-018-1434-8
34. M. Wang, Z. Yang, Z. Song, Q. Wang, *J. Heterocycl. Chem*. **2015**, *52*, 907–910. **DOI:**10.1002/jhet.2132
35. A. R. Moosavi-Zare, M. A. Zolfigol, S. Farahmand, A. Zare, A. R. Pourali, R. Ayazi-Nasrabadi, *Synlett*. **2014**, *25*, 193–196. **DOI:**10.1055/s-0033-1340088
36. M. Karim Koshteh, M. Bagheri, *J. Mex. Chem. Soc*. **2017**, *61*, 28–34. **DOI:**10.29356/jmcs.v61i1.118
37. X. Zhao, L. Zeng, N. Hosmane, Y. Gong, A. Wu, *Chin. Chem. Lett*. **2019**, *30*, 87–89. **DOI:**10.1016/j.cclet.2018.01.028
38. K. K. Gangu, S. N. Maddila, S. Maddila, S. B. Jonnalagadda, *J. Alloys Compd*. **2017**, *690*, 817–824. **DOI:**10.1016/j.jallcom.2016.08.201
39. H. Saeidian, F. Moradnia, *Quarterly J. Iran. Chem. Commun*. **2017**, *5*, 252–261.
40. J. Shen, X. Li, W. Huang, N. Li, X. Ye, *J. Mate. Res*. **2014**, *29*, 2211. **DOI:**10.1557/jmr.2014.250
41. J. Etemad Gholtash, M. Farahi, B. Karami, M. Abdollahi, *Acta Chim. Slov*. **2020**, *67*, 866–875. **DOI:**10.17344/acsi.2020.5825
42. S. H. Choi, Korean *J. Mater. Res*. **2018**, *28*, 371–375. **DOI:**10.3740/MRSK.2018.28.7.371
43. U. Kurtan, R. Topkaya, A. Baykal, M. S. Toprak, *Ceram. Int*. **2013**, *39*, 6551–6558. **DOI:**10.1016/j.ceramint.2013.01.088
44. M. Nasrollahzadeh, M. Bagherzadeh, H. Karimi, *J. Colloid Interface sci*. **2016**, *465*, 271–278. **DOI:**10.1016/j.jcis.2015.11.074
45. K. Sinkó, E. Manek, A. Meiszterics, K. Havancsák, U. Vainio, H. Peterlik, *J. Nanopart. Res.* **2012**, *6*, 1–4.
46. Y. Zhang, Z. Yang, B. P. Zhu, W. Yu, S. Chen, X. F. Yang, F. Jin, J. Ou-Yang, *Ceram. Int*. **2014**, *40*, 3439–3443. **DOI:**10.1016/j.ceramint.2013.09.087

Povzetek

Dušikove heterociklične spojine so predmet številnih raziskav, saj izkazujejo široko biološko in farmacevtsko uporabnost. V tej študiji smo sintetizirali pet- in šestčlenske dušikove obročne sisteme s pomočjo "one-pot" multikomponentne reakcije z uporabo kobaltovega feritnega nanokatalizatorja, dopiranega z aluminijem. Nanokatalizator smo pripravili z metodo so-obarjanja iz ustreznih kovinskih soli. Rezultati kažejo, da je katalizator visoko učinkovit in da omogoča tvorbo željenih produktov z visokimi izkoristki in čistotami. Enostavnost izvedbe ter preprostost čiščenja produktov, krajši reakcijski časi, milejši reakcijski pogoji, enostavnost ločbe in ponovna uporabnost katalizatorja so glavne odlike tega katalizatorja.